# Structure of Fluorinated Side-Chain Smectic Copolymers: Role of the Copolymerization Statistics

**G. de Crevoisier,[†,§] P. Fabre,[†,⊥] L. Leibler,[†] S. Tencé-Girault,[*,†] and J. M. Corpart[‡]**

*UMR 167 CNRS-ATOFINA-ESPCI, 10, rue Vauquelin 75031 Paris Cedex 05, France, and CAL-ATOFINA, 95 Rue Danton, 92303 Levallois-Perret, France*

*Received March 15, 2001; Revised Manuscript Received January 14, 2002*

ABSTRACT: Side-chain fluorinated copolymers present very specific wetting and tacking properties that are strongly related to their organization. We have studied the structure of these systems by X-ray scattering in the liquid crystalline regime, as a function of the ratio of fluorinated groups on one hand and of the copolymerization statistics on the other. The structures obtained are always highly ordered and exhibit a smectic B type organization, where the two types of pendant groups are able to crystallize independently. However, packing differences appear for copolymers with different chain statistics due to the existence of microphase separation between the side groups. The roles of these parameters on phase transitions, periodicity, and degree of crystallinity of the polymers are discussed. Their behavior with temperature, important for applications, is also studied.

## Introduction

Side-chain liquid crystalline polymers have been the subject of much interest, for both fundamental and applied reasons. Since they present an original architecture, they can potentially display interesting new structures on one hand, while on the other, they are expected to exhibit properties that can lead to new applications such as long-term memory devices or nonlinear optics. In fact, other unexpected applications were found for that type of system: when enough fluorine is present in one of the pendant groups, side-chain copolymers organize in such a way that very hydrophobic and oleophobic properties appear. As a consequence, these types of copolymers are used as antistain coatings. More recently, other specific properties have been reported[1] for these systems, such as a nonsticky to sticky transition related to a structure change with temperature. For both these reasons, it was tempting to study the organization of fluorinated copolymers, when varying their composition, as a first step to relating their structure to their properties. Moreover, another recent study[2] has led to the original result that it was possible, in these systems, to vary the copolymerization statistics from statistical to rather blocky, by changing the type of synthesis from solution to emulsion. With this system, it is thus possible to study how both the composition and the copolymerization statistics of the chain influence the structure, leading to results that will a priori be valid for a whole class of side-chain copolymers.

The copolymers studied bear two types of pendant moieties: one fluorinated group and one alkyl group. As explained, their ratio as well as their distribution along the chain was varied, and the two homopolymers were also studied for comparison. To understand the copolymer structure, a knowledge of the monomer's miscibility is also relevant: for this reason, we determined their phase diagram. The impact of temperature on their structure and in particular the phase transitions of the copolymers are also studied in this paper, since they represent very important information as far as their surface (wetting) or volume (stickiness) properties are concerned. The study was realized with both small-angle (SAXS) and wide-angle (WAXS) X-ray scattering experiments and with DSC for the phase transitions.

In the first part, we describe the experimental results for the two homopolymers as well as the phase diagram of the mixture of the two monomers. We then discuss what can be expected for copolymers and describe the experimental results when varying the fluorine ratio and the polymerization statistics. We then present a possible organization of the systems as a function of these two main parameters.

## Experimental Section

**Materials.** Two main monomers were used in this study, the structures of which are given in Figure 1. The alkyl monomer is an equimolar mixture of stearyl ($m = 17$) and palmityl ($m = 15$) methacrylate; for simplicity, we will hereafter call this MAS. The fluorinated acrylic monomer, which we call AC8*n*, is a mixture of acrylates with fluorinated side chains of different lengths: $n = 6$ (1%), $n = 8$ (65%), $n = 10$ (25%), and $n = 12$ (9%). We will sometimes refer to the pure $n = 8$ fluorinated compound, which we call AC8. Hydroxyethyl methacrylate (HEMA) was also used as a hydrophilic monomer. All these monomers were provided by ATOFINA and used without further purification. The polymerization initiators used were 2,2′-azobis(2-amidinopropane) hydrochloride and 2,2′-azobis(isobutyronitrile). These were provided by ATOFINA. The solvents used were acetone and butyl acetate provided by Aldrich. All these compounds were used without further purification.

**Preparation and Characterization of the Polymers.** All syntheses were carried out in a 1 L reactor fitted with an anchor agitator, a double thermoregulated jacket, and a sweep of nitrogen.

In the case of synthesis in solution, 425 g of butyl acetate and 75 g of AC8n and MAS monomers were introduced into the reactor in varying proportions, corresponding to the composition of the copolymer that was targeted. For a par-

† UMR CNRS-ATOFINA-ESPCI.
‡ CAL-ATOFINA.
§ Present address: ATOFINA Japan, Kyoto Technical Center SCB#3, Kyoto Research Park,1 Awatacho, Chudoji, Shimigyo-ku Kyoto 600-8815 Japan.
⊥ Present address: CRPP, Av. Dr Schweitzer, 33600 Pessac, France.
* To whom correspondence should be addressed.

10.1021/ma010459t CCC: $22.00 
Published on Web 04/04/2002

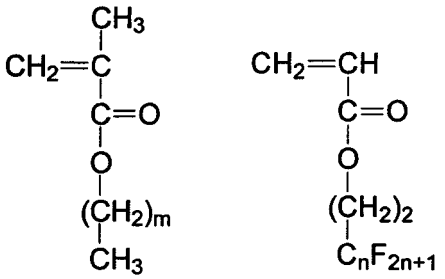


**Figure 1.** Chemical structure of the two monomers MAS and AC8*n* (see experimental part for *n* and *m* values).

**Table 1. A Typical Recipe for Emulsion Polymerization**

| ingredients | amount (g) |
|---|---|
| water | 375 |
| acetone | 106.8 |
| trimethyloleylammonium chloride | 13.2 |
| polyoxyethylenenonylphenol (HLB = 15.0) | 12.1 |
| monomers (AC8*n*/MAS/HEMA)[a] | 174.5 |
| dodecylmercaptan | 0.3 |

[a] The monomer feed composition is variable depending on the copolymer we want to synthesize. HEMA rate is constant (10 molar %).

ticular copolymer, HEMA was used as third monomer at a ratio of 10% molar, with the synthesis protocol remaining identical. The medium was then inerted by a bubbling of nitrogen and raised to 70 °C. Polymerization was initiated by the addition of 1.5 g of 2,2′-azobis(isobutyronitrile) in solution in a minimal quantity of butyl acetate. At the end of 6 h of polymerization, a limpid solution was obtained, of yellow color, containing the copolymer. The solution remained clear after cooling to ambient temperature. The copolymers were recovered by precipitation in acetone. They were then washed with ethanol and dried in a vacuum until constant weight. It should be noted that with this synthesis technique we were unable to synthesize highly fluorinated copolymers of AC8*n* and MAS, where the concentration of AC8*n* was higher than 70% molar. In fact, for these rates of fluorinated monomer, we observed a phase separation during synthesis.

In the case of synthesis in emulsion, all compounds were introduced into the reactor. A typical recipe is provided in Table 1. The respective ratios of AC8*n* and MAS monomers were variable depending on the composition of the copolymers targeted. In all cases, HEMA was incorporated into the mixture of monomers at a ratio of 10% molar. After inerting with nitrogen and heating to 65 °C, polymerization was initiated by addition of 2 g of 2,2′-azobis(2-amidinopropane) hydrochloride. After 3 h of polymerization, we obtained latexes that were perfectly stable in storage. The copolymers were recovered, like their homologues prepared in solution, by precipitation in acetone. They were then washed twice in distilled water and once in ethanol and then dried in a vacuum at 45 °C until constant weight.

The homopolymers of MAS, AC8, and AC8*n* (respectively PMAS, PAC8, and PAC8n) were synthesized in solution in butyl acetate. The PMAS was recovered under the same conditions as the copolymers. The PAC8 and PAC8*n* precipitated during synthesis. They were recovered by filtration, washed with ethanol, and dried in a vacuum at 45 °C.

At ambient temperature, the synthesized homopolymers and copolymers showed themselves in the form of a white powder.

The molar mass and polydispersity of such opolymers are delicate to determine. GPC in THF was realized on some copolymers synthesized in solution, with polystyrene as a reference. The average molar masses obtained were lying between 14 000 and 45 000, with a large polydispersity. We considered these results just as an indication that the length of the chains is small for the solution copolymers. For the emulsion synthesis, it is well-known that the chains are in general much longer, leading to molar masses ranging between $10^5$ and $5 \times 10^5$ g/mol.

To determine the statistics of the chains for each type of synthesis, we used a $^{13}C$ NMR experiment,[2] and we just summarize the main points here. From the spectra, the concentration in several types of triads was determined and fitted with the classical Markovian model for chain statistics and the reactivity ratios found in the literature: the fits for a statistical copolymerization were in excellent agreement with the experimental results for polymers synthesized in solution. For polymers synthesized in emulsion, there was a deviation from a statistical composition, with a large excess in homotriads. The larger ratio homotriads/heterotriads could be associated with the presence of more blocky structure along the polymer chains in the case of emulsion process. The exact determination of the length of those blocks remains very delicate, and we also cannot exclude the possible existence of mainly fluorinated or hydrogenated macromolecules.

Below, for reasons of simplicity, we will use the term blocky for emulsion polymer and statistical for solution ones, although one should bear in mind that the emulsion polymers are at best multiblocks with blocks of which the length is moreover unknown. In the text, the copolymers will be called -*b*- for "blocky" or -s- for "statistical", and their composition will be characterized by the molar fractions in fluorinated pendant groups: a copolymer 30-s will thus be statistical and composed of 30% fluorinated groups and 70% alkyl groups. The different compositions studied are 20-s, 30-s, 40-s, 50-s, 60-s, and 70-s for the statistical copolymers and 20-b, 35-b, and 58-b for the blocky ones. Note that for emulsion copolymers there is always 10% of HEMA as an additional polar monomer so that for example 58-b means 58% of AC8n, 32% of MAS, and 10% of HEMA. To check that this termonomer had little influence on the structure, an additional copolymer was synthesized in solution, with 10% of HEMA: this statistical terpolymer has the same composition as the emulsion copolymer 58-b and is called 58-s-32/10.

**Experimental Techniques and Sample Preparation.** The different techniques we used to determine the copolymer structures are optical microscopy, DSC, wide-angle (WAXS), and small-angle (SAXS) X-ray scattering.

Optical microscopy clearly showed that the samples were birefringent and undergoing phase transitions, but the nature of the phases could not be determined from the observed textures. No thermal treatment, such as annealing, was able to clear up the textures. In addition, as far as copolymers synthesized in emulsion were concerned, thermal treatments always induced the occurrence of a white aspect of the sample, due to high turbidity. We did not however observe any specific structures, such as heterogeneous textures or aggregates, at a microscopic scale.

For the DSC experiments, after a preliminary heating at high temperature, a first cooling and second heating, from which the different parameters are extracted, were realized at 10 °C/min.

For X-ray experiments, we used two different setups (SAXS and WAXS) with the same rotating anode generator (RU-200, Rigaku Co. Ltd.) using Cu Kα radiation. Small-angle X-ray diffraction patterns were recorded on a linear position sensitive detector (LPS 50 INEL) and wide-angle X-ray diffraction patterns on a curve position sensitive detector (CPS 120 INEL). The samples are prepared by increasing temperature well above any transition temperature and, after a 10 min wait at high temperature, by cooling them at room temperature at 10 °C/min. The sample is then heated at 10 °C/min at the desired experimental temperature and left to equilibrate for 10 min at this temperature before starting the experiment. X-ray experiments done with a 2D detector as well as optical microscopy allowed us to check that the orientation of the samples was of a powder type after the procedure we used.

## Monomers and Homopolymers

**Structure and Phase Transitions of the Homopolymers.** Homopolymers similar to ours have been

described in the literature. Since the pendant groups we use present some polydispersity in length, we checked whether this polydispersity had an influence on their structure.

**a. PMAS.** The structures of the two alkyl homopolymers with $m = 15$ and $m = 17$ have been described in the literature. The homopolymers with $m = 15$ and $m = 17$ present a smectic B phase of periodicity respectively 28 and 30.4 Å,[3−7] with peaks at wide angles corresponding to a hexagonal lattice of parameter 4.7 Å.[8,9] The pendant groups are packed perpendicularly to the layers[1] and interdigitated, which favors their crystallization.

For PMAS, we find a lamellar periodicity of 29.7 Å, and we observed a crystalline Bragg peak at 4.10 Å, corresponding to an hexagonal lattice parameter of 4.7 Å superimposed on an amorphous halo. These results are in agreement with what is found in the literature, showing that there is little influence of the polydispersity in length of the pendant groups. From the half-maximum width of the peaks, one can evaluate the different correlation lengths of the system with the Scherrer expression for perfect crystals:[10]

$$\xi = \frac{0.9\lambda}{\Delta 2\theta \cos \theta}$$

With the wide angle Bragg peak, we evaluate the correlation length of the crystals $\xi_{MAS}$ at 78 Å, corresponding to about 16 monomers; on the other hand, the correlation length of the layers $\xi_L$ obtained from the small-angle Bragg peak is larger, roughly equal to 400 Å, i.e., extending over 10−15 layers. Both these lengths are rather small, indicating a rapid loss of correlation in this smectic B polymer.

The size of one completely extended monomer is 23 Å, which is significantly smaller than the periodicity of 29.7 Å of the smectic. Thus, we can conclude that there is a double layer structure with the pendant groups either tilted or interdigitated. By comparison with literature, it seems reasonable to consider that the intermediary distance for the periodicity comes from an interdigitation of the groups,[2] rather than a tilt. Moreover, the packing density is also a result of the competition between the area occupied by the pendant groups and the density of these groups along the chain: the distance between groups on the lattice (4.7 Å) being almost equal to twice their distance along the chain (2.54 Å); this means that two successive pendant groups alternate on each side of the chain and thus belong to two different layers when crystallized. The resulting structure for PMAS is represented in Figure 2.[11,12]

DSC experiments show that the transition temperature of the smectic B phase to an isotropic phase is $T_i = 33$ °C, with an enthalpy of transition $\Delta H = 76$ J/g. This value is also in agreement with literature.

**b. PAC8 and PAC8*n*.** In literature, the organization for PAC8 is described as a smectic B with a periodicity of 33.3 Å.[13−15] For the same reasons as in PMAS, the structure proposed is a succession of bilayers of pendant groups coming alternatively from two different chains. However, contrary to PMAS, the observed periodicity is exactly twice the size of one extended monomer. This means that the groups do not interpenetrate, probably due to the large size and the rigidity of perfluorinated groups. The lattice parameter is 5.7 Å.

DSC together with X-ray experiments shows that there is a transition from the smectic B to an isotropic phase for PAC8 and PAC8*n*. However, the width of the peak for PAC8*n* is much larger than for PAC8, because of the polydispersity of the side groups. Indeed, the melting temperature of perfluorinated chains increases very rapidly with the chain length in this range (22 °C per carbon atom).[16] The transition temperature, defined as the maximum of the peak, is increased between PAC8 and PAC8*n* from 78 to 103 °C due to the longer chains. From X-rays, we measure a periodicity of respectively 32.4 and 36.9 Å and a Bragg peak at 4.95 Å, leading to a hexagonal lattice parameter of 5.7 Å in agreement with literature, superimposed on an amorphous halo. The breadth of the peaks, characterizing the correlation length of the systems, is very different between PAC8 and PAC8*n*. From the lamellar peak, we obtained the correlation length between layers: $\xi_L$ which is equal to 800 Å for PAC8 and 300 Å for PAC8*n*, showing that the smectic order is inhibited by the polydispersity of the side groups. In the crystalline layers, the correlation length of crystallized domains of AC8 or AC8*n* is $\xi_{AC8} \approx 170$ Å, corresponding to about 30 monomers, and $\xi_{AC8n} \approx 200$ Å, corresponding to about 35 monomers, showing no significant difference. The structure of PAC8*n* deduced from X-rays experiments is shown in Figure 2.

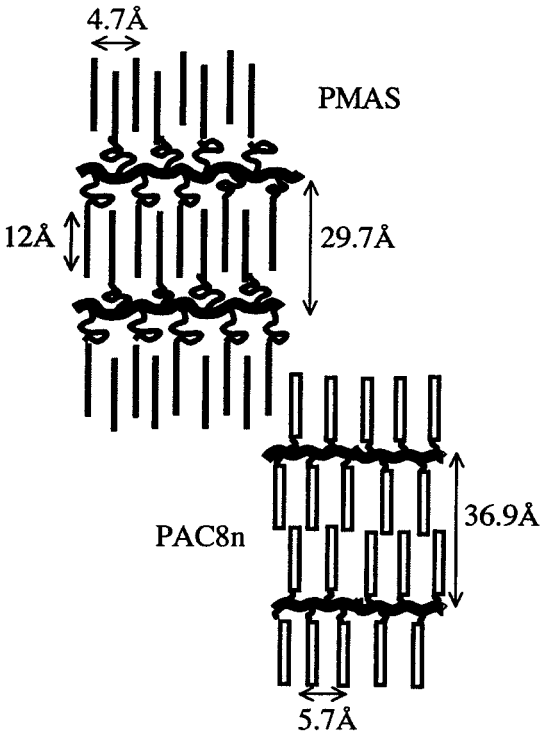


**Figure 2.** Schematic representation of the organization of PMAS and PAC8*n*.

In conclusion, the two homopolymers possess a smectic B structure of bilayers with a slight interdigitation of the pendant groups for PMAS. They both present a phase transition to an isotropic phase. No major difference was found between the "polydisperse" homopolymer PAC8*n* and the "monodisperse" PAC8, besides smaller interlayer correlation lengths.

**Compatibility between Monomers: Experimental Results.** To quantify the compatibility between monomers, which is a useful information for the copolymers structure, we studied the phase diagram of a mixture of MAS and AC8*n*. For compositions lying between 20% and 80% of AC8*n*, the mixture of the two monomers introduced in closed tubes were putted in an

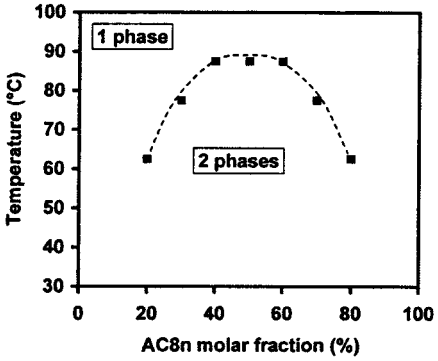


**Figure 3.** Phase diagram of a mixture of the two monomers MAS and AC8*n*.

oven. At 120 °C all the solutions are homogeneous; then we decrease the temperature down to the temperature where a tube becomes turbid, indicating the separation in two phases. We report these temperatures vs the molar fraction of the solutions for establishing the phase diagram displayed in Figure 3. The important point for the following is that, since all our X-rays experiments were realized below 80 °C, the monomers were always incompatible in the temperature range where the copolymers were studied.

## Copolymers

**Side-Chain Copolymers: Role of Monomer Compatibility and Chain Statistics.** Compared to homopolymers, the chemical ingredients driving the organization of linear copolymers are the ratio between monomers, their compatibility, their architecture, and the copolymerization statistics. Monomer compatibility is characterized by the Flory parameter $\chi$, which describes the enthalpy cost of A−B contacts relative to A−A or B−B. The copolymerization between monomers prevents them from undergoing a complete segregation and can lead to microphase separation. For chains with simple architecture such as diblock or triblock copolymers, this microphase separation leads to formation of ordered mesophases, such as layers in diblock copolymers for example. The morphology diagrams of such block or regularly grafted systems are fairly well understood.[17−20] For statistical copolymers the situation is more complex, and the question of existence of ordered mesophases and of the role of chemical disorder is still open.

The case of side-chain copolymers with two different pendant groups A and B is slightly different from chains with one pendant group because of their architecture. The side chains possess an additional degree of freedom for the two pendant groups which can rotate around the main chain, giving extra organization possibilities to the copolymer.

Depending on the monomers A and B compatibility, different types of situations can thus arise for side-chain copolymers: for a statistical copolymerization and compatible monomers, a smectic structure with a periodicity intermediary between that of the two monomers appears, whereas for incompatible monomers, the system structures with a "double" period corresponding to the sum of the periods of the two monomers. Changing the statistics of copolymerization has no influence in the case of compatible monomers that can still structure with the same period. For incompatible monomers, though, a change in the statistics of the chain influences

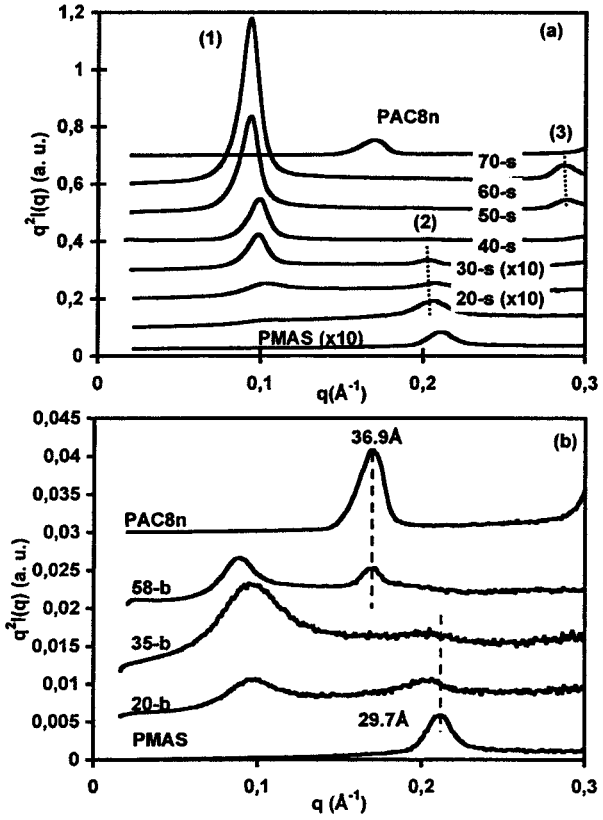


**Figure 4.** Small-angle X-ray spectra for homo- and copolymers at room temperature for (a) solution synthesis and (b) emulsion synthesis.

the structure: for instance, in the extreme case of perfect blockiness, the two separate blocks will structure with their own period, leading to the appearance of the periods of the homopolymers in the copolymer structure. Many studies have been made on diblock copolymers of the type liquid crystalline-*b*-coil leading to very different types of packing.[21−25] In the few cases studied of a blocky copolymer with two side-chain liquid crystalline groups, each block organizes as in the homopolymer.[26,27] A few studies also deal with statistical side-chain liquid crystalline copolymers and give the following results: depending on the monomer compatibility, the smectic period is "simple" or "double", and the number of phase transitions to the isotropic phase is different.[22,28−30]

**Copolymer Structure. a. Statistical Copolymers.** Figure 4a presents the SAXS spectra for statistical copolymers as a function of fluorinated moieties ratio. We have also reported, in this figure, both spectra observed for PAC8*n* and PMAS. We observe for the two homopolymers only one peak in this range of wave vector at 0.17 $Å^{-1}$ for PAC8*n* and 0.21 $Å^{-1}$ for PMAS. But, for all intermediate compositions, we observe smectic Bragg peaks labeled by (1) for the first, (2) for the second, or (3) for the third order of diffraction, at a different wave vector than for homopolymers. This means that the copolymers still arrange with a smectic order but with a different periodicity around 60 Å. The periodicity of the smectic phase vs fluorine ratio reported in Table 2 is close to the sum of the periods of the two homopolymers. Unfortunately, we were unable to study the area of lower concentrations of fluorine (AC8*n* concentration less than 20% molar), and we therefore do not know from what concentration of fluorine this new organization appears. It would prob-

**Table 2. Powder X-ray Diffraction Data and DSC Phase Transition Temperatures for the polymers**

| samples | lamellar period (Å) | | normalized WAXS intensity[a] | | crystallite size (Å) | | melting temp (°C) | | normalized enthalpy[b] (J/g) | |
|---|---|---|---|---|---|---|---|---|---|---|
| | | | | Homopolymers | | | | | | |
| PMAS | 29.7 | | 0.44 | | 78 | | 33 | | 76 | |
| PAC8*n* | | 36.9 | | 0.36 | | 200 | | 103 | | 21 |
| | | | | Statistical Copolymers | | | | | | |
| 20-s | 61.7 | | 0.28 | 0.04 | 78 | 56 | 31.6 | | 47 | |
| 30-s | 62.0 | | 0.31 | 0.07 | 74 | 74 | 29.3 | | 48 | |
| 40-s | 63.6 | | 0.31 | 0.11 | 69 | 49 | 33.0 | | 80 | |
| 50-s | 63.5 | | 0.39 | 0.32 | 72 | 135 | 35.0 | 57.0 | 57 | 10 |
| 60-s | 66.7 | | | | 59 | 158 | 35.0 | 60.0 | 58 | 14 |
| 70-s | 66.2 | | 0.20 | 0.43 | 39 | 190 | 25.0 | 63.0 | 40 | 19 |
| | | | | Blocky Copolymers | | | | | | |
| 20-b | 30.6−64.2 | | 0.44 | 0.10 | 71 | 83 | 29.5 | 33.1 | 74 | |
| 35-b | 30.6−63.5 | | 0.44 | 0.20 | 61 | 86 | 29.4 | 55.3 | 74 | 2 |
| 58-b | 30.5−70.1−36.9 | | 0.46 | 0.46 | 81 | 120 | 29.2 | 62.2 | 79 | 6 |

[a] The intensity has been normalized by the total intensity scattered at wide angles and by the fraction of monomers of each species. [b] Enthalpy normalized by the molar fraction in the copolymer.

ably be interesting to conduct some further experiments in this area. For highly fluorinated copolymers (above 70% molar of AC8*n*), we again have no data. However, the situation is more complicated. In fact, the solvent used for syntheses, butyl acetate, is no longer capable of solubilizing the copolymers formed, and polymerization becomes precipitant. For obvious reasons, we have not explored this area.

The relative intensity of the successive order of diffraction changes with composition, indicating an evolution of the electronic density in the lamellae. Nevertheless, evaluation and quantification of the electronic density profile is very difficult. It is also surprising that the intensity of the first-order peak continuously increases with the composition, between 20 and 70% of AC8*n*, without any maximum at the composition 50/50. It is perhaps an indication that this lamellar organization concerns an ever increasing volume when the molar fraction of AC8*n* increases. It is worth noticing that the correlation length between layers of the copolymers $\xi_L$, extracted from the width of the peaks, is around 400 Å, i.e., the same as in homopolymers: this however represents half less in terms of number of layers, since the periodicity is twice as large.

WAXS experiments are summarized in Figure 5a: the same two peaks as for homopolymers are observed, meaning that the two monomers are able to crystallize separately in their own lattice. There are thus two different lattices in the system. On the other hand, the crystalline peaks have a comparable width and thus comparable correlation lengths as the two homopolymers. Indeed, for 50-s copolymer, for instance, the correlation lengths are $\xi_{AC8n} = 170$ Å and $\xi_{MAS} = 130$ Å. It is reasonable to assume that the copolymer crystallizes in a smectic B phase with small crystallites. The relative intensity of the crystalline peaks is varying continuously with fluorine composition, and they superimpose on an amorphous contribution. To quantify the evolution of crystallinity of each monomer with composition and separate the three contributions, we used a classical procedure[31] for evaluating amorphous scattering and crystallinity from the WAXS spectra. The result is shown in Figure 6a, where we have plotted the relative integrated intensity of the crystalline peak ($I_{AC8n}/I_{total}$) or ($I_{MAS}/I_{total}$) of each monomer normalized by the fraction of monomers of each species as a function of fluorine ratio. We have reported this crystallinity and also the size of crystallized domains extracted from the peak width calculated with the Scherrer expression for perfect crystals in Table 2. The evolutions of crystallinity and size of crystallites will be discussed in the following, together with DSC experiments.

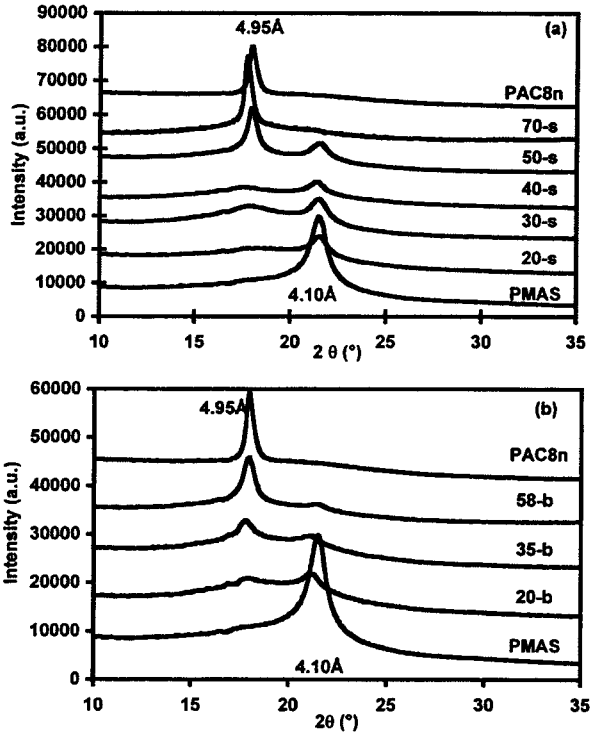


**Figure 5.** Wide-angle X-ray spectra for homo- and copolymers at room temperature for (a) solution synthesis and (b) emulsion synthesis.

These results thus show that the general structure of statistical copolymers is that of a smectic B, with a crystallization of both types of monomers in the layers; their periodicity is the sum of the periodicity of the homopolymers.

**b. Nonstatistical Copolymers.** The same experimental data as for statistical copolymers have been obtained for blocky copolymers and are represented together in the same figures, in part b. This allows us to point out the similarities and differences between the two types of structures.

The SAXS experiments show a very different behavior than for statistical copolymers: three different periods are observed, with values of around 30, 37, and 65 Å.

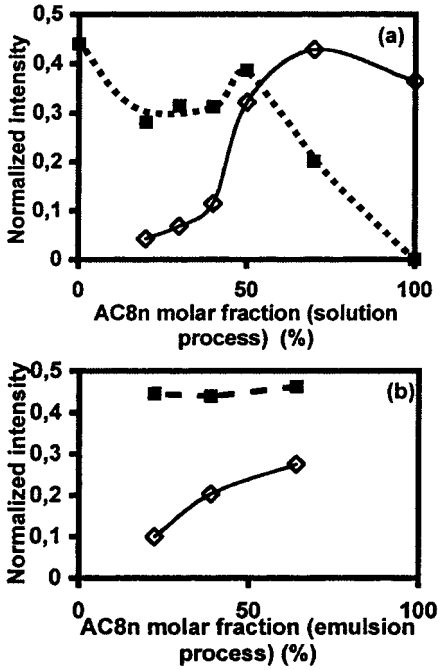


**Figure 6.** Crystalline peaks intensity vs AC8*n* molar fraction for (a) solution synthesis and (b) emulsion synthesis. The intensity has been normalized by the total intensity scattered at wide angles and by the fraction of monomers of each species (full symbol on dotted line for PMAS and open symbol on solid line for PAC8*n*; lines are guides for the eyes).

Thus, the blocky copolymers present three types of organization at the same time, corresponding to the two smectic phases of the homopolymers, plus the same "double" period as in statistical copolymers. Moreover, the relative intensities of the "double" period peak in the two types of copolymers are very different, leading to the conclusion that there is a much smaller part of the blocky copolymers that organizes into the double period phase.

The difference is much less dramatic on the WAXS spectra (Figure 5b), where one observes again the two types of crystalline peaks. The variation with fluorine ratio of the domain sizes is only slightly different from statistical copolymers.

The evolution of crystallinity with the number of monomers of each type is different for statistical and nonstatistical copolymers. For blocky copolymers, the increase in crystallinity of the fluorinated monomer is almost linear whereas the crystallinity of the alkyl one is constant (Figure 6b). For statistical copolymers, the situation is more complex and the behavior of crystallinity of fluorinated and alkyl monomers is nonmonotonic (Figure 6a). Concerning the domain sizes, it remains constant with the increase of the fluorine ratio for the alkyl crystal whereas it constantly increases for the fluorinated crystal. Let us also notice that the domain size is of the same order of 100 Å in the two types of systems, except for fluorine-rich statistical copolymers where it is twice as large.

**c. Structure vs Copolymerization Statistics.** As a first conclusion, it seems that statistical as well as blocky side-chain copolymers are both able to organize into crystallized smectic B phases. The difference lies in the period of the smectic organization that, for statistical systems, is unique whereas the periods of the homopolymers also appear for the more blocky ones.

We have compared the organization of the 58-s-32/10 copolymer with that of the 60-s and detect no effect from the presence of HEMA on the lamellar organization of the copolymer. We can therefore consider that the structural differences observed between copolymers prepared in solution and in emulsion are not due to the presence of this termonomer.

Thus, depending on the type of copolymerization, several situations are a priori possible. In our case, the existence of a "double" period leads to the conclusion that the monomers segregate, in agreement with their phase diagram. The "double" period corresponds to a packing of layers of different composition. The layers contain alternatively more fluorinated moieties and more alkyl moieties, the relative composition of the layers depending on the overall fluorine ratio. The existence of three periods for blocky copolymers shows that there is a strong composition heterogeneity, with more blocky and more statistical regions.

**Phase Transitions and Evolution of the Structure with Temperature.** The transition temperatures obtained from DSC experiments are reported in Table 2 for statistical and blocky polymers. The general evolution of these temperatures is similar, but depending on the copolymer, there is one or two transitions with temperature between the smectic B and the isotropic phase. Moreover, the lower transitions always occur at a similar temperature, close to the smectic B to isotropic transition temperature of PMAS. On the contrary, the higher transition temperature is close to the PAC8*n* smectic B−isotropic transition temperature for fluorine-rich copolymers and is decreasing when the fluorine ratio is decreasing in the copolymer, down to the PMAS transition temperature.

To understand how the smectic B with two different lattices organization loses its order, DSC experiments are not sufficient, and the study of the evolution of X-rays spectra with temperature was necessary. These experiments were done, with statistical copolymers, for two different fluorine ratios, 30-s and 60-s, and for one block copolymer, 58-b. As a reference, we also studied the homopolymers.

For PAC8, we observed a simultaneous decrease of the intensities of the smectic and crystalline Bragg peaks at the temperature determined by the DSC experiment. The behavior of PMAS is the same and leads to the conclusion that these polymers have no smectic A phase.

The results for 30-s and 60-s copolymers are given in Figure 7. We have reported the intensity of lamellar and crystalline peaks normalized to the intensity observed at 20 °C. First, we should note that the two copolymers present two transitions contrary to what was observed with DSC where copolymer 30-s only had one (Table 2): this method is thus more sensitive than DSC. Second, the disappearance of the lamellar peak always occurs at a temperature close to the temperature of disappearance of one of the two crystalline peaks; however, it occurs close to the alkyl crystals peak in the case of 30-s and close to the fluorine crystals peak in the case of 60-s. We interpret the disappearance of the peak as a disappearance of the lamellar order, although the contrast of the lamellar phase, which was already low, certainly decreases even further when approaching the transition. In this case, we can deduce from the experiments that the disappearance of the lamellar order occurs concomitantly with the melting of the

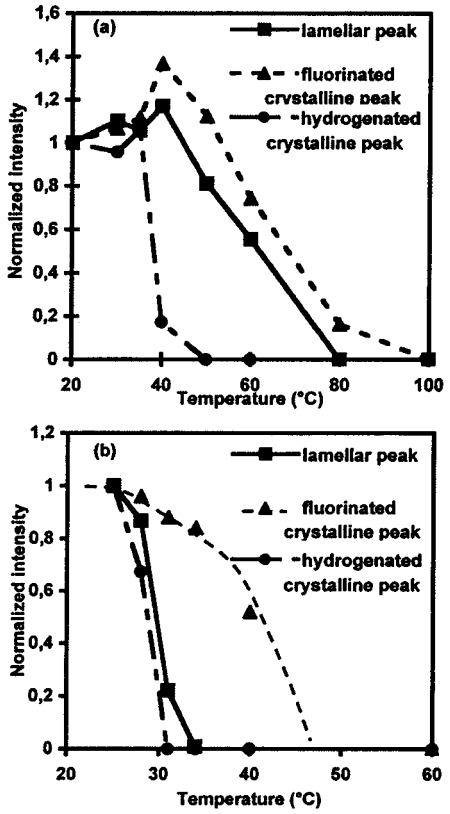


**Figure 7.** Evolution of lamellar and crystalline peaks intensity with temperature for (a) 60-s and (b) 30-s.

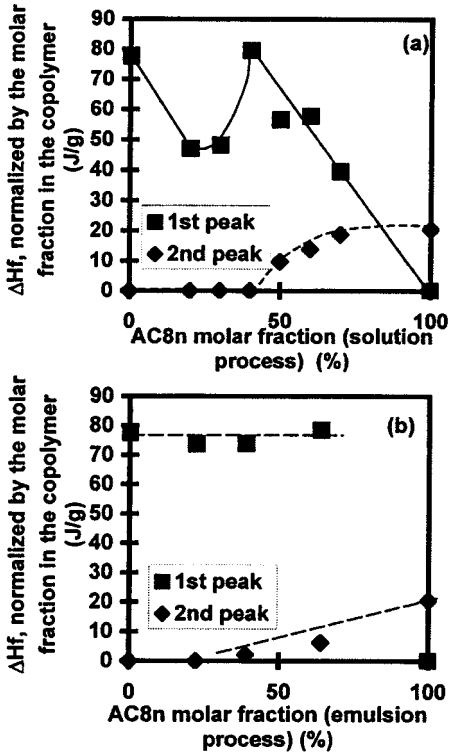


**Figure 8.** Evolution of the enthalpy changes for the melting of the two types of crystals vs AC8*n* molar fraction for (a) solution synthesis and (b) emulsion synthesis.

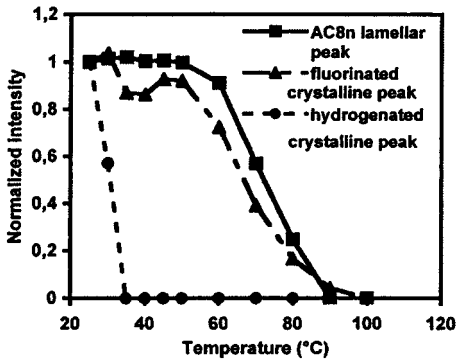


**Figure 9.** Evolution of lamellar and crystalline peaks intensity with temperature for 58-b.

monomer in excess, showing that the major monomer is responsible for the presence of the smectic order; the minor monomer melts independently of the smectic structure. Two different cases are thus possible: for a MAS major copolymer, at a temperature close to the pure PMAS transition temperature, the smectic B phase disappears, while the AC8*n* crystals are still present in the system until a higher melting temperature. To the contrary, for an AC8*n*-rich copolymer, the MAS crystals melt first, while the smectic B phase remains with the fluorine crystals until a higher transition temperature where the system becomes isotropic.

The variation of the transition temperatures observed by DSC shows that the behavior of the copolymers remains driven to a large extend by the homopolymer's transition temperatures, indicating that the two organizations present are neither totally independent nor completely correlated. In Figure 8a,b, the enthalpy values of the two transitions are plotted with fluorine ratio: it is remarkable that these curves can be exactly superimposed on Figure 6a,b which represent the amount of crystallinity of the two monomers calculated from WAXS spectra.

Concerning the block copolymer 58-b, the WAXS spectra give access to the behavior of the two crystalline peaks together with the lamellar period of the fluorinated homopolymer (Figure 9). The data show a decrease of the alkyl crystals peak intensity at a first temperature, followed at a higher temperature by a simultaneous decrease of the fluorinated crystals and of the fluorinated homopolymer smectic peak intensities. SAXS experiments would be necessary to fully understand the behavior of the system, since it would display the double period evolution with temperature. However, the partial information obtained with WAXS is consistent with the fact, deduced previously, that the blocky copolymer is composed of regions of the homopolymers type.

## Discussion

**Summary of the Experimental Results.** In statistical as well as in blocky copolymers, we observed the appearance of a new period corresponding to the sum of the periods of homopolymers, together with the crystallization of both monomers in their original lattice, whatever the composition. However, for blocky copolymers, the periodicity of homopolymers also appears in the spectra, meaning that some regions of the system are crystallized like homopolymers.

The overall crystallinity and the size of crystalline domains are not dramatically different for the same composition between the statistical and the blocky copolymers. On the other hand, the amount of crystallinity of each type of monomer largely depends on its ratio in the chain, although not in a linear way.

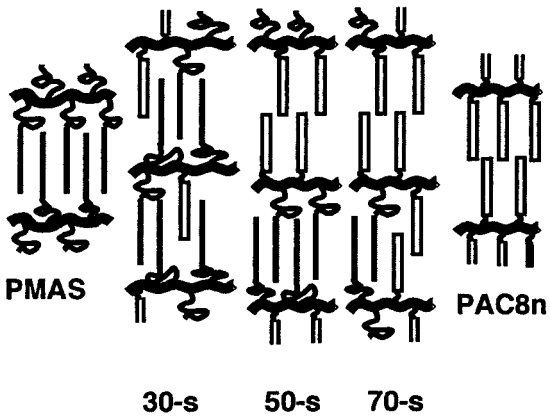


**Figure 10.** Schematic representation of solution copolymer organization vs fluorine content.

Concerning the transition to an isotropic structure for statistical copolymers, this always occurs in two stages. These two stages depend on which is the major monomer. Indeed, the major monomer drives the loss of smectic order, so that the melting of the smectic B occurs close to the AC8*n* melting temperature for AC8*n*-rich copolymers and almost at the MAS melting temperature for MAS-rich copolymers. In the case of AC8*n*-rich copolymers, there is thus a very specific succession of phases: above what could be called a "bicrystallized" smectic B phase, there is an intermediary smectic B phase, which could be called "hemicrystallized", where only the fluorine layers are crystallized, then the system becomes isotropic. Notice that these copolymers never exhibit smectic A phases. If the double period lamellae disorganize at the melting temperature of the excess monomer in the case of statistical copolymers, the situation is a little more complex for nonstatistical copolymers, where, in addition, the disorganization of homopolymer-type regions occurs in the same way as in homopolymers.

Below, we relate these data to the monomer organization at the chain scale, as a function of the copolymerization statistics.

**Structure of the Copolymers vs Fluorine Ratio. a. Solution Copolymers.** In a very rough approximation, we consider that the system diminishes its enthalpy of mixing by segregating the two monomers in the following way: one layer is filled up with the excess monomer, while the other layer contains a mixture of the remaining excess monomer and the minority one. Of course, this optimal packing is not always possible, depending on the chain statistics, the monomer volume and mobility, and the flexibility of the chain. Moreover, the thermal composition fluctuations that necessarily occur will contribute to a deviation from this packing rule. Nevertheless, following the argument of maximal segregation, we have represented the structure of copolymers in line with the fluorine ratio in Figure 10.

In this model, the symmetric copolymer 50-s is as organized as the homopolymers since each layer is "pure": this is indeed in agreement with our results, where in Figure 6a one can see that the amount of crystallinity in this copolymer is almost equal for each monomer to the crystallinity of the corresponding homopolymer, when renormalized with the molar fraction in pendant groups. Moreover, if we assume that MAS, when it is in a mixed layer, is no longer able to crystallize, we are able to explain the nonmonotonic behavior of its crystallinity when fluorine is added.

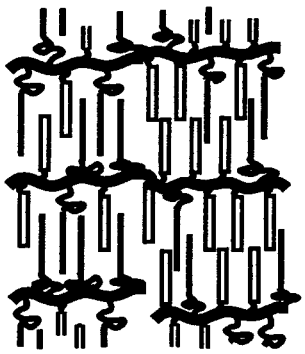

**Figure 11.** Schematic representation of emulsion copolymer organization. The variation of fluorine content will only modify the proportion of the two types of crystals.

Indeed, for a copolymer of composition $f$ in AC8*n*, the fraction of MAS monomers packed in a "pure" layer is equal to $(0.5/1 - f)$: this expression is in agreement, where $f < 0.5$, with the evolution of the peak intensities, which is proportional to the amount of crystallinity, represented in Figure 6a. However, the behavior of MAS crystallinity for fluorine compositions larger than 50% cannot be explained by this argument. More generally, the asymmetric features of copolymers with respect to a fluorine composition larger or smaller than 50% cannot be explained without involving a different behavior for alkyl and fluorinated monomers. Also, the melting temperature for fluorine crystallites drops when the fluorine ratio is decreased, in contrast to the alkyl crystallites melting temperature, which remains constant. These two features could be linked to the difference in the enthalpy of melting of fluorinated and alkyl chains.

**b. Emulsion Copolymers.** Copolymers synthesized in emulsion can be described by the superimposition of homopolymer-type regions and of zones similar to those present in statistical copolymers: this is schematically shown in Figure 11. It is very difficult in this system with three different types of phases, probably separated by interphases of continuously varying compositions, to predict any fluorine ratio dependency of the parameters. It is thus difficult to quantitatively compare our data to the model for the structure.

## Conclusion

In this paper, we have studied the organization of liquid crystalline copolymers as a function of the polymerization statistics, which in our case can be simply controlled by the type of synthesis: solution or emulsion. The copolymers carry two types of highly incompatible pendant groups, one fluorinated and one alkyl group, in varying ratios. The originality of this study is thus to vary both the composition of the copolymer and the copolymerization statistics. Whatever the chain statistics and composition in monomers, the copolymers organize in a very structured phase, composed of a smectic whose layers are crystallized in two different lattices. The copolymer synthesized in solution, whose monomer distribution along the chain is statistical, leads to a smectic phase with a single periodicity roughly equal to the sum of the periodicities of the two homopolymers. To the contrary, three different periodicities appear in the blockier copolymers obtained from a synthesis in emulsion: the two homopolymer periodicities and their sum. These structural differences are very important as far as the applications of these

systems are concerned. Indeed, the type of crystallization of the systems is known to play a role in the hydrophobic and oleophobic properties of a coating of a copolymer as well as in its adhesive characteristics.[3] For example, depending on the statistics of the chain, the kinetics of reorganization[2] of the groups at the interface is extremely different, leading to very versatile surface tension values. Also, the type of phase in which the system crystallizes has been shown to be responsible for the capacity for tackiness of these systems.[1] The knowledge of the parameters driving the structure can thus help to predict, and then to design, the most appropriate system for a given property.

**Acknowledgment.** The authors thank A. Kowalik and A. C. Gayon for the synthesis of the copolymers, A. Ibos and P. Decourval for the X-ray experiments, B. Lanteri for the DSC experiments, R. P. Eustache and J. C. Chiajese for the NMR experiments, and C. Gay for many fruitful discussions.

## References and Notes

(1) de Crevoisier, G.; Fabre, P.; Corpart, J. M.; Leibler, L. *Science* **1999**, *285*, 1246.
(2) de Crevoisier, G. Thèse de Doctorat, Université Pierre et Marie Curie, Paris VI, 1999.
(3) Hsieh, H. W. S.; Post, B.; Morawetz, H. *J. Polym. Sci., Polym. Phys. Ed.* **1976**, *14*, 1241.
(4) Platé, N. A.; Shibaev, V. P.; Petrukhin, B. S.; Kargin, V. A. *J. Polym. Sci., Part C* **1968**, *23*, 37.
(5) Greenberg, S. A.; Alfrey, T. *J. Am. Chem. Soc.* **1954**, *76*, 6280.
(6) Platé, N. A.; Shibaev, V. P.; Petrukhin, B. S.; Zubov, Yu. A.; Kargin, V. A. *J. Polym. Sci., Part A1* **1971**, *9*, 2291.
(7) Duda, G.; Schouten, A. J.; Arndt, T.; Lieser, G.; Schmidt, G. F.; Bubeck, C.; Wegner, G. *Thin Solid Films* **1988**, *159*, 221.
(8) Shibasaki, Y.; Fukuda, K. *Therm. Anal., Proc. Int. Conf. 7th* **1982**, *2*, 1517.
(9) Kaufman, H.; Sasher, A.; Alfrey, T.; Faukuchen, I. *J. Am. Chem. Soc.* **1948**, *70*, 3147.
(10) Guinier, A. Théorie et technique de la radiocristallographie, Dunod, 1956.
(11) A model of the electronic density along the groups, based on the fit of the maximum intensity of the Bragg peaks with a superposition of sinusoidal functions (see ref 12), allows to calculate the distance $l$ over which the layers are interpenetrated: $l = 12$ Å.
(12) Davidson, P.; Strzelecki, L. *Liq. Cryst.* **1988**, *3*, 1583.
(13) Mélas, M. Thèse de Doctorat, Université de Montpellier II, 1995.
(14) Volkov, V. V.; Platé, N. A.; Takahara, A.; Kajiyama, T.; Amaya, N.; Murata, Y. *Polymer* **1992**, *33*, 1316.
(15) Shimizu, T.; Tanaka, Y.; Kutsumizu, S.; Yano, S. *Macromol. Symp.* **1994**, *82*, 173.
(16) Meakawa, T.; Kamata, S.; Matsuo, M. *Proc. XIIIth Symposium on Fluorine Chemistry*, Bochum, 1991.
(17) Leibler, L. *Macromolecules* **1980**, *13*, 1602.
(18) Bates, F. S.; Frederickson, G. H. *Phys. Today* **1999**, 32−38.
(19) Benoit, H.; Hadziioannou, G. *Macromolecules* **1988**, *21*, 1449.
(20) Milner, S. T. *Macromolecules* **1994**, *27*, 2333.
(21) Mao, G. P.; Ober, C. K. *Acta Polym.* **1997**, *48*, 405.
(22) Pugh, C.; Kiste, A. L. *Prog. Polym. Sci.* **1997**, *22*, 610.
(23) Antonietti, M.; Forster, S.; Micha, M. A.; Oestreich, S. *Acta Polym.* **1997**, *48*, 262.
(24) Krupers, M.; Möller, M. *Macromol. Chem. Phys.* **1997**, *198*, 2163.
(25) Ober, C. K.; Wang, J. G.; Mao, G. P. *Macromol. Symp.* **1997**, *118*, 701.
(26) Percec, V.; Lee, M. *J. Mater. Sci., Pure Appl. Chem.* **1992**, *A29*, 723.
(27) Poser, S.; Arnold, M.; Fischer, H. *Eur. Polym. J.* **1996**, *32*, 1169.
(28) Jordan, E. F.; Artymyshyn, B.; Speca, A.; Wrigley, A. N. *J. Polym. Sci., Part A1* **1971**, *9*, 3349.
(29) Neumann, H. J.; Jarek, M.; Hellman, G. P. *Macromolecules* **1993**, *26*, 2489.
(30) Alig, I.; Jarek, M.; Hellmann, G. P. *Macromolecules* **1998**, *31*, 2245.
(31) Murthy, N. S.; Minor, H. *Polymer* **1990**, *31*, 996.

MA010459T